RAPID MAGNITUDE DETERMINATION FOR EARLY WARNING CONSIDERING THE TIME-DEPENDENCE OF P-WAVE GROWTH AND ITS APPLICATION

S. Noda[(1)]

[(1)] *Assistant Senior Researcher, Railway Technical Research Institute, noda.shunta.59@rtri.or.jp*

Abstract

To issue an alert using earthquake early warning (EEW) at the earliest opportunity, rapid determination of earthquake magnitude (*M*) is critical because ground motion distribution can be computed from the source parameters (hypocenter or epicenter and *M*) using a ground motion prediction equation. This study tests a *M* determination approach recently proposed to check if it is applicable to the single station method used in the Shinkansen (high-speed rail in Japan) EEW system. In the approach, the intercept of ground motion prediction equation for determining *M* is set as a function of time while it is conventionally constant, suggesting that the new method can be easily installed to the algorithm because only the intercept parameter update is required to use it. The analysis demonstrates that the proposed approach allows us to measure *M* more rapidly than the conventional method without loss of accuracy even for the single station method. We conclude that the proposed approach can improve the performance of the EEW system.

Keywords: earthquake early warning; magnitude; initial rupture; scaling relation

1. Introduction

Earthquake early warning (EEW) system can provide an alert for strong shaking before it starts in order to allow people and systems to take actions to protect life and property [e.g., 1]. The Japanese high-speed rail (Shinkansen) is equipped with its own EEW system (the Shinkansen EEW system) that can decelerate or halt running trains to reduce their risks during a large event when a stop signal is issued from a seismometer of the system [2]. The first Shinkansen EEW system, Urgent Earthquake Detection and Alarm System (UrEDAS), started its operation in 1992 [3] and was replaced with a new system in 2004 [2]. The Railway Technical Research Institute (RTRI) updates the system even after the replacement to improve its performance [e.g., 4, 5].

Commonly, EEW algorithms determine source parameters (source location, and earthquake magnitude: *M*) in real time from the observed seismic data while the rupture is still in progress [e.g., 6]. Ground motion distribution can be computed using a ground motion prediction equation (GMPE) from the parameters (i.e., hypocenter or epicenter and *M*) so that warning information is issued to the area where the estimated motion is stronger than a pre-defined threshold. In the Shinkansen EEW system, an epicenter location is obtained using the "C-Δ" algorithm that enables us to determine the location at every single station (the single station method) [2, 5]. The single station method estimates *M* as well after locating the epicenter in order to determine which running trains need to be stopped [7]. This demonstrates that the fast *M* determination is a key to ensure the safety of railway when an earthquake occurs.

Historically, *M* was defined as a value that was proportional to observed displacement amplitude at a given distance (local magnitude: M_L) [8], and then other definitions of earthquake magnitude were proposed, such as, moment magnitude M_W [9]. Even in the many of current EEW systems, *M* can be determined from displacement amplitude of a body wave using a relation with *M* [e.g., 10, 11, 12], e.g.,

$$\log Disp_c = \log Disp + \alpha \times \log R = \beta \times M + \gamma \qquad (1),$$

where *Disp* is displacement amplitude, $Disp_c$ is displacement amplitude corrected by distance, *R* is hypocentral distance and α, β, and γ are coefficients determined for the relation. Note that Eq. (1) is the simplest form for GMPE. Hereafter, *M* determination based on a GMPE is referred to as the GMPE approach, which is used also in the single station method of the Shinkansen system.

Even though the GMPE approach is commonly used in EEW algorithms, we note that it has a technical limitation in terms of the estimation speed of *M*. That is, the final *M* cannot be estimated until the peak amplitude is observed because a GMPE is applied before the arrival of the peak amplitude to estimate *M* while the event is still underway. Colombelli and Zollo [13] and Noda et al. [14] demonstrated that it typically required about 1.5 s, 3–4 s, and 10 s after the P onset, respectively, for *M* 5, *M* 6, and *M* 7 until the peak amplitude arrives (either in acceleration or in displacement), which are consistent with typical earthquake rupture durations [e.g., 15]. This suggests that it is impossible to know the final *M* of earthquakes before the rupture is terminated if this limitation is correct, although that is still a controversial problem [e.g., 16, 17, 18]. It is critical, however, to determine *M* faster to further improve the safety of running trains.

This article first reviews a paper [19] that investigated if it was possible to overcome this technical limitation and then looks at another study [20] that proposed a new technique to estimate *M* more rapidly than using the conventional GMPE approach. Finally, this study demonstrates that the proposed technique is useful for the single station method in the Shinkansen EEW system and that it can upgrade the performance of the system.

2. Scaling relation between *M* and the departure time from P-wave similar growth

This chapter introduces Noda and Ellsworth [19] who examined characteristics of initial P-wave records observed at K-NET stations (operated by the National Research Institute for Earth Science and Disaster Resilience; NIED). Noda and Ellsworth [19] analyzed the absolute displacement of initial P waves averaged in bins partitioned by distance and *M*, and showed that the initial P-wave data for $4.5 \le M_W \le 8.7$ started

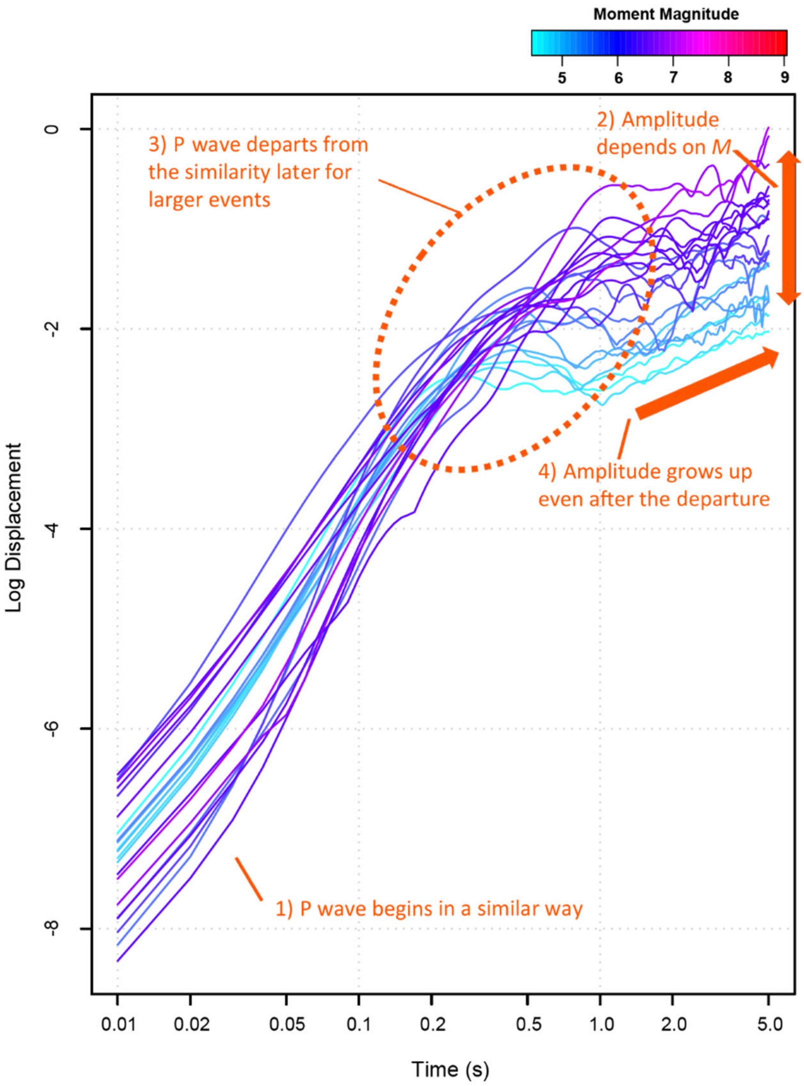

Fig. 1 – Four characteristics in initial P-wave growth shown by Noda and Ellsworth [19].

similarly (i.e., there was no significant dependence of the initial P-wave displacement on M_W; Fig. 1). This is consistent with a number of previous studies [e.g., 21, 22, 23, 24]. Noda and Ellsworth [19] also found that the departure from the similarity was later for larger earthquakes and that it occurred before the arrival of the peak amplitude. A scaling relation was proposed between the departure time (T_{dp}) and M_W (Fig. 2):

$$M_W = 2.29 \times \log T_{dp} + 5.95 \quad (2).$$

T_{dp} is about 0.4, 1.1, and 2.9 s, respectively, for M_W 5, 6, and 7, which is significantly shorter than the typical peak amplitude arrival indicated in Chapter 1 (i.e., T_{dp} is approximately 30% of typical source duration). Note that it seems the scaling relation is established up to M7-class earthquakes according to Noda and Ellsworth [19].

Although Noda [25] discussed how the scaling relation could be explained in terms of the physical mechanism, that still remains unclear. Nevertheless, the scaling relation can be considered in the GMPE approach of EEW as shown in the next chapter.

3. Magnitude determination considering the departure time for the GMPE approach

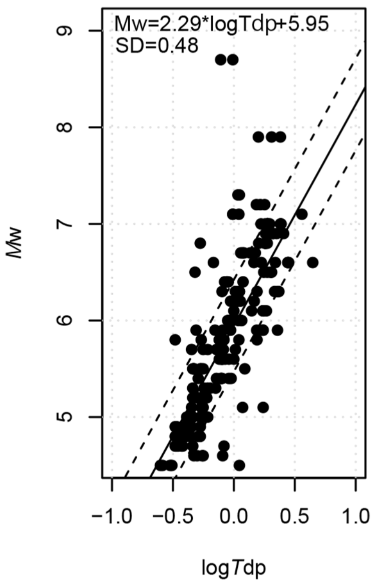

Fig. 2 – Relationship between $\log T_{dp}$ and M_W presented by Noda and Ellsworth [19]. Black solid and dashed lines show the regression relation and its standard deviation (SD), respectively.

Based on the finding of the scaling relation between T_{dp} and M_W, Noda and Ellsworth [20] proposed a new technique that enabled us to infer M faster than the conventional GMPE approach.

The proposed technique employs Eq. (1) in which the coefficients α, β and γ are usually constant. The coefficient α is associated with the geometrical spreading while the coefficients β and γ control the relationship between M and displacement corrected by distance. The β value corresponds with the slope of the relationship so that it adjusts the correlation between them and the γ value represents the intercept of the relationship. In Fig. 3, the slope of the relationship (black solid lines) is initially small, suggesting that P wave begins similarly as shown in the previous chapter. The slope increases with time, that is, the correlation becomes stronger.

The new technique uses constant β because the scaling relation between M_W and T_{dp} (Eq. 2) demonstrates that only measurements made at times after T_{dp} are significant in terms of the correlation between M_W and the maximum amplitude (red dots in Fig. 3). On the other hand, γ is set as a function of time (γ[T]) because the maximum displacement grows as time increases as can be seen in Fig. 3. For fixed β, when γ[1.00 s] is determined for example, M_W is 5.95 for T_{dp} = 1 s evaluated from Eq. (2), so that we use only the maximum displacements from events of magnitude less than M_W 5.95 because earthquakes smaller than M_W 5.95 at T = 1 s have already passed T_{dp}. In Fig. 3, the red dashed lines show the equations for β (constant) and γ[T] proposed in the study. The coefficients are summarized in Table 1.

Although Noda and Ellsworth [20] concluded that the proposed technique was effective to improve the speed of the M determination without loss of accuracy, the analysis evaluated the median of the M estimates determined at the five closest stations for each event hypocenter. In Chapter 4, we check if the proposed technique is applicable to the single station method used in the Shinkansen EEW algorithm.

Table 1 – The coefficients of Eq. (1) obtained in Noda and Ellsworth [20].

***T* (s): Time from the P onset**	**α**	**β**	**γ**
1.00	1.33	0.68	-3.30
1.25			-3.25
1.50			-3.22
1.75			-3.17
2.00			-3.15
2.50			-3.09
3.00			-3.02
4.00			-2.95

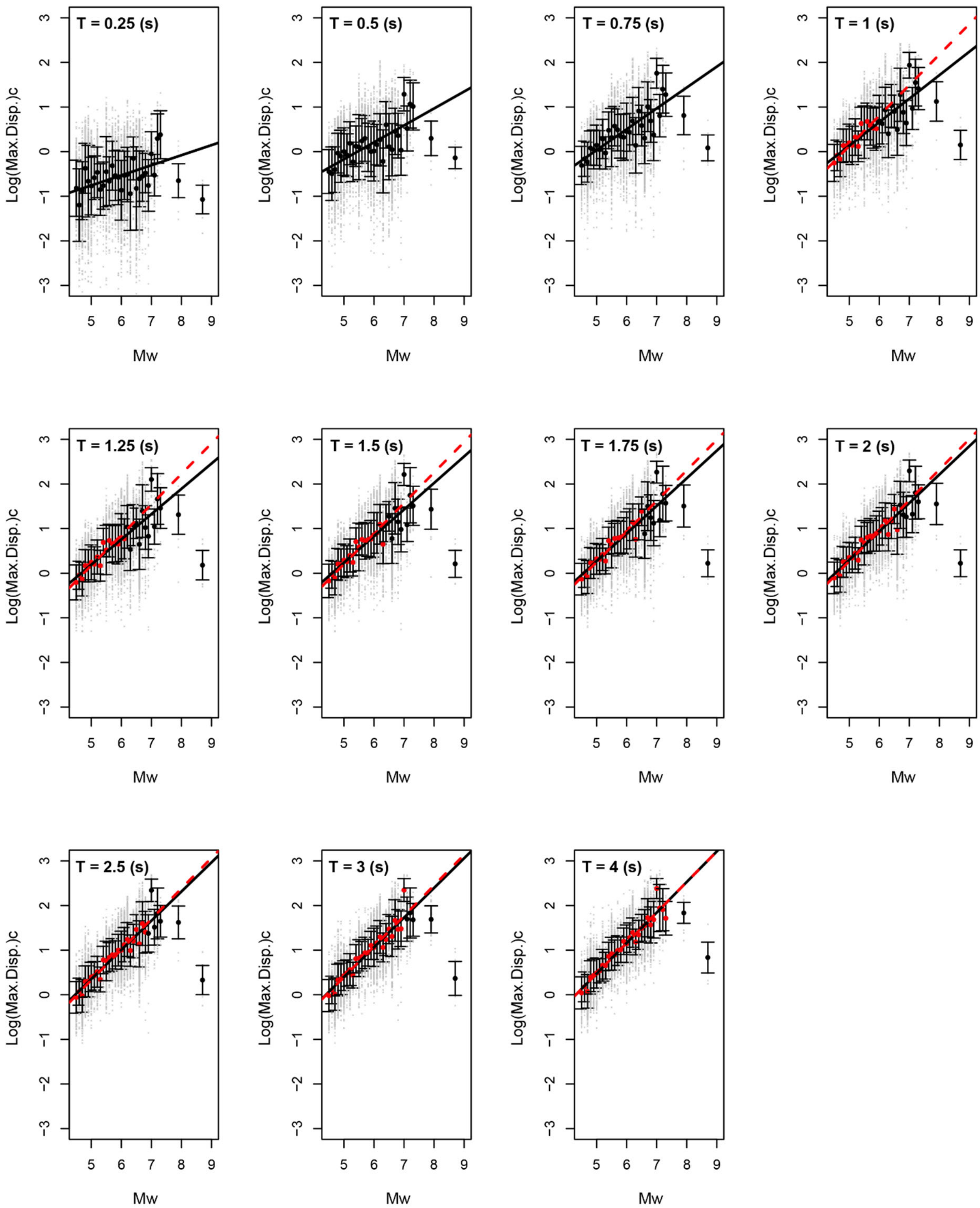

Fig. 3 – Relationship between M_W (horizontal axis) and the logarithm of the maximum absolute displacement corrected by hypocentral distance (vertical axis) shown by Noda and Ellsworth [20]. Gray points show the data observed at every station in the dataset. Black or red dots and error bars show the average and the standard deviation computed for each M_W bin. Black solid lines are the regression lines using the data of both black and red dots. Red dots are the data used to determine $\gamma[T]$. Red dashed lines show the regression lines obtained from the red dots using the constant slope ($\beta = 0.68$).

4. Application to the Shinkansen EEW algorithm

In this chapter, we test M estimates (M_{est}) computed at each single station from the technique proposed by Noda and Ellsworth [20]. We use the same dataset with Noda and Ellsworth [20]. Fig. 4 shows the locations of the 149 earthquakes with $4.5 \leq M_W \leq 9.0$ and with the source depth $\geq$ 60 km. We select observations with hypocentral distance less than 200 km. This results in the 7,437 waveforms recorded at K-NET stations. We analyze the initial 4-second data after the P onset with the frequency range of 0.075 – 3 Hz. The running maximum of the absolute displacement is applied to the proposed M determination method.

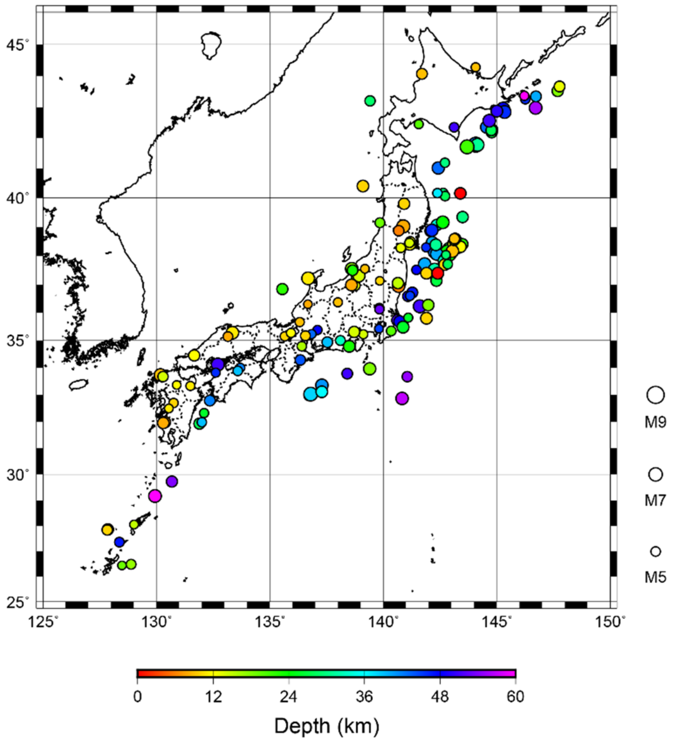

Fig. 4 – Distribution of hypocenters analyzed in this study.

Fig. 5 presents the relationship between M_W (horizontal axis) and $M_{est} - M_W$ (vertical axis) at each time T (time after the P onset). By the way of comparison, the gray and black points are obtained from the conventional (constant $\gamma[T = 4\ s]$) and the proposed (time-dependent $\gamma[T]$) methods, respectively. The blue squares and the red triangles show the means of $M_{est} - M_W$ in M_W 0.5 magnitude units, respectively for the gray and black points, and the error bars indicate their standard deviations. This result demonstrates that: the scatters of the residual (i.e., the standard deviation) between M_{est} and M_W are equivalent between the one from the conventional (the blue square's error bars) and from the proposed techniques (the red triangle's error bars) even in the case of using the single station method: and that the final M should be estimated faster using the proposed method than the conventional one because the red triangles (estimated from the new technique) are closer to zero even at earlier times than the blue squares (from the conventional method). We conclude thta these are consistent with the conclusions of Noda and Ellsworth [20].

An important advantage of the proposed approach is that it can be easily installed with the Shinkansen EEW system because all we need to do to use it is to change the intercept parameter (γ) from constant to time-dependent in the relationship between M and displacement. We conclude that the proposed method is useful for the Shinkansen EEW system to reduce the risks of the bullet trains during big earthquakes.

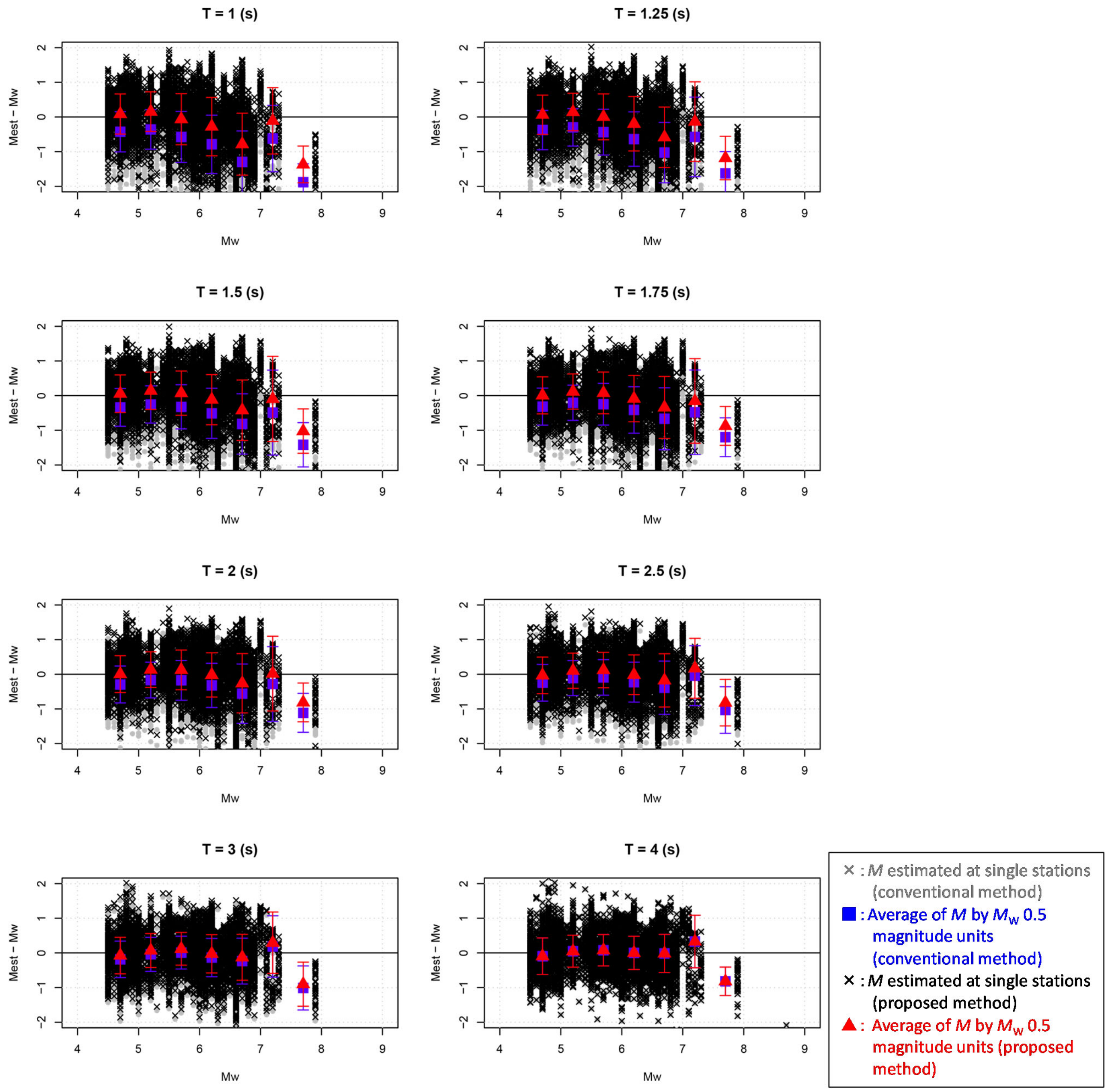

Fig. 5 – Distribution at each T between M_W (horizontal axis) and M_{est} (M estimates determined at each single station) – M_W (vertical axis). Black solid line indicates the reference of $M_{est} - M_W = 0$. Black and gray points show the results from the time-dependent intercept $\gamma[T]$ and the constant $\gamma[T = 4\ s]$, respectively. The averages of $M_{est} - M_W$ by M_W 0.5 magnitude units are shown by the red triangles (for the black points: the proposed method) and by the blue squares (for the gray points: the conventional method), and the error bars indicate their standard deviations.

5. Summary

This study tested a M determination approach newly proposed by Noda and Ellsworth [20] for the single station method which is utilized in the Shinkansen EEW algorithm in order to improve its performace. To estimate M faster, the proposed technique applies time-dependent intercepts to the relationship between M and displacement while the conventional method used a constant one. The analysis showed that the new method can infer the final *M* more rapidly than the conventional method without losing the estimation accuracy. We conclude that the proposed technique can improve the safety of running trains during earthquakes.

6. Acknowledgements

The author is grateful to the National Research Institute for Earth Science and Disaster Resilience for enabling him to use the waveform records. The author used the Generic Mapping Tools [26] to draw Fig. 4.

7. References

[1] Hoshiba M, Kamigaichi O, Saito M, Tsukada S, Hamada N (2008): Earthquake early warning starts nationwide in Japan. *EOS Trans*, *AGU*, **89**, 73-74.

[2] Yamamoto S, Tomori M (2013): Earthquake Early Warning system for railways and its performance. *Journal of JSCE*, **1**, 322-328.

[3] Nakamura Y (1988): On the urgent earthquake detection and alarm system (UrEDAS). *Proc. 9th World Conf. Earthq. Eng.*, **7**, 673-678.

[4] Noda S, Yamamoto S, Sato S, Iwata N, Korenaga M, Ashiya K (2012): Improvement of back-azimuth estimation in real-time by using a single station record. *Earth Planets Space*, **64**, 305–308.

[5] Iwata N, Yamamoto S, Korenaga M, Noda S (2015): Improved algorithms of seismic parameters estimation and noise discrimination in earthquake early warning. *Quarterly Report of RTRI*, **56** (4), 291-298.

[6] Kamigaichi O, Saito M, Doi K, Matsumori T, Tsukada S, Takeda K, Shimoyama T, Nakamura K, Kiyomoto M, Watanabe Y (2009): Earthquake early warning in Japan: Warning the general public and future prospects. *Seism. Res. Lett.*, **80** (5), 717-726.

[7] Nakamura H, Iwata N, Ashiya K (2005): Statistical relationships between earthquake disaster and seismic parameters used for train operation control after earthquake. *RTRI Report*, **19** (10), 11-16 (in Japanese).

[8] Richter CF (1935): An instrumental magnitude scale. *Bull. Seism. Soc. Am.*, **25**, 1-32.

[9] Kanamori H (1977): The energy release in great earthquakes. *J. Geophys. Res.*, **82**, 2981-2987.

[10] Odaka T, Ashiya K, Tsukada S, Sato S, Ohtake K, Nozaka D (2003): A new method of quickly estimating epicentral distance and magnitude from a single station record. *Bull. Seism. Soc. Am.*, **93** (1), 526-532.

[11] Wu YM, Zhao L (2006): Magnitude estimation using the first three seconds P-wave amplitude in earthquake early warning. *Geophys. Res. Lett.,* **33**, L16312, doi:10.1029/2006GL026871.

[12] Kuyuk HS, Allen RM (2013): A global approach to provide magnitude estimates for earthquake early warning alerts. *Geophys. Res. Lett.*, **40**, 6329–6333, doi:10.1002/2013GL058580.

[13] Colombelli S, Zollo A (2015): Fast determination of earthquake magnitude and fault extent from real-time P-wave recordings. *Geophys. J. Int.*, **202**, 1158-1163.

[14] Noda S, Yamamoto S, Ellsworth WL (2016): Rapid estimation of earthquake magnitude from the arrival time of the peak high-frequency amplitude. *Bull. Seism. Soc. Am.*, **106** (1), 232-241.

[15] Kanamori H, Brodsky E (2004): The physics of earthquakes. *Rep. Prog. Phys*., **67**, 1429-1496.

[16] Olson EL, Allen RM (2005): The deterministic nature of earthquake rupture. *Nature*, **438**, 212–215.

[17] Rydelek P, Horiuchi S (2006): Is earthquake rupture deterministic?. *Nature*, **442**, doi:10.1038/nature04963.

[18] Iio Y (2009): Earthquake nucleation process: Does the initiation of earthquake rupture know about its termination?. *Encyclopedia of Complexity and Systems Science*, edited by R. A. Meyers, Springer, New York, NY, U.S.A., **3**, 2538–2555.

[19] Noda S, Ellsworth WL (2016): Scaling relation between earthquake magnitude and the departure time from P wave similar growth. *Geophys. Res. Lett.,* **43**, doi:10.1002/2016GL070069.

[20] Noda S, Ellsworth WL (2017): Determination of earthquake magnitude for early warning from the time dependence of P-wave amplitudes. *Bull. Seism. Soc. Am.*, **107** (4), 1860-1867.

[21] Abercrombie R, Mori J (1994): Local observations of the onset of a large earthquake: 28 June 1992 Landers, California. *Bull. Seismol. Soc. Am.*, **84** (3), 725-734.

[22] Mori J, Kanamori H (1996): Initial rupture of earthquakes in the 1995 Ridgecrest, California sequence. *Geophys. Res. Lett.,* **23***,* doi:10.1029/96GL02491.

[23] McLaskey GC, Lockner DA (2014): Preslip and cascade processes initiating laboratory stick slip. *J. Geophys. Res. Solid Earth*, **119**, doi:10.1002/2014JB011220.

[24] Meier MA, Heaton T, Clinton J (2016): Evidence for universal earthquake rupture initiation behavior. *Geophys. Res. Lett.*, **43**, doi:10.1002/2016GL070081.

[25] Noda S (2018): Statistical characterization of P-wave growth for earthquake early warning. *Quarterly Report of RTRI*, **59** (2), 128-134.

[26] Wessel P, Smith WHF (1998): New, improved version of generic mapping tools released. *EOS Trans*, *AGU*, **79**, 579.

